A role for atmospheric CO_2 in preindustrial climate forcing

Thomas B. van Hoof*†‡, Friederike Wagner-Cremer†, Wolfram M. Kürschner†, and Henk Visscher†

*TNO Geological Survey of the Netherlands, Princetonlaan 6, 3584 CB Utrecht, The Netherlands; and †Palaeoecology, Institute of Environmental Biology, and Laboratory of Palaeobotany and Palynology, Utrecht University, Budapestlaan 4, 3584 CD Utrecht, The Netherlands

Communicated by David L. Dilcher, University of Florida, Gainesville, FL, August 21, 2008 (received for review March 3, 2007)

Complementary to measurements in Antarctic ice cores, stomatal frequency analysis of leaves of land plants preserved in peat and lake deposits can provide a proxy record of preindustrial atmospheric CO_2 concentration. CO_2 trends based on leaf remains of *Quercus robur* (English oak) from the Netherlands support the presence of significant CO_2 variability during the first half of the last millennium. The amplitude of the reconstructed multidecadal fluctuations, up to 34 parts per million by volume, considerably exceeds maximum shifts measured in Antarctic ice. Inferred changes in CO_2 radiative forcing are of a magnitude similar to variations ascribed to other mechanisms, particularly solar irradiance and volcanic activity, and may therefore call into question the concept of the Intergovernmental Panel on Climate Change, which assumes an insignificant role of CO_2 as a preindustrial climate-forcing factor. The stomata-based CO_2 trends correlate with coeval sea-surface temperature trends in the North Atlantic Ocean, suggesting the possibility of an oceanic source/sink mechanism for the recorded CO_2 changes.

carbon cycle | global warming | past millennium | stomata

It is increasingly realized that temperature-sensitive proxy records inferred from tree rings, lake deposits, and historical documents corroborate occurrences of significant preindustrial air-temperature fluctuations during the last millennium (1–5). Also, the *Fourth Assessment Report* of the Intergovernmental Panel on Climate Change (IPCC) (6) now cautiously presents a whole range of historical temperature reconstructions instead of favoring the earlier "hockey-stick" graph of the *Third Assessment Report* of the IPCC (7). The reconstructed fluctuations show largely differing amplitudes and timing. It is obvious that individual proxy temperature curves are not parallel to the generally accepted atmospheric CO_2 curve for the last 1,000 years, which is characterized by a very low degree of preindustrial variability. This curve is based on CO_2 records from Antarctic ice cores, which suggest that until the onset of industrialization in the 19th century, atmospheric CO_2 concentration (expressed as mixing ratio) varied by not more than 12 parts per million by volume (ppmv) (8–12). Although modest negative CO_2 anomalies have been associated with the Little Ice Age (10, 11, 13, 14), the *Fourth Assessment Report* treats such variation as an insignificant forcing mechanism for generating preindustrial air-temperature changes (6), especially when compared with effects of changes in solar irradiance and explosive volcanic activity (15–18).

Estimates of preindustrial CO_2 levels are available not only from Antarctic ice but also from leaves of land plants preserved in peat and lake deposits. Particularly in a wide variety of woody plants, the genetically controlled inverse relationship between numbers of leaf-stomata (gas exchange pores) and ambient CO_2 concentration during the growth period (19) permits detection and quantification of past CO_2 changes by analyzing time-series data on stomatal frequency. The *Fourth Assessment Report* recognizes that stomatal frequency may provide reasonable constraints on past CO_2 variations on long geological time scales (10^5 to 10^8 years), but does not appreciate the applicability of this proxy for identifying decadal to millennial scale CO_2 changes during the Holocene Epoch (6). Yet, the integrity of short-term leaf-based CO_2 changes has been verified by fine-resolution analysis of the lifetime CO_2 responsiveness of individual trees (20) and by numerous other response curves based on well dated herbarium material and subfossil leaves, which consistently mimic the ongoing CO_2 increase apparent from Mauna Loa instrumental monitoring (21–24). Reproducibility of leaf-based CO_2 reconstructions is further demonstrated by coeval stomatal frequency records of taxonomically, geographically, and ecologically contrasting tree species, which confirm a coupling between CO_2 anomalies and early Holocene cooling events (25–28).

For the last millennium, pronounced preindustrial CO_2 variability has been reconstructed on the basis of needles of *Tsuga heterophylla* (western hemlock) from Mount Rainier, Washington, USA (29), and leaf remains of *Quercus robur* (English oak) from the southeastern part of the Netherlands (27, 30). The timing of the detected CO_2 changes is in good agreement with perturbations observed in Antarctic ice core records. Remarkably, however, reconstructed amplitudes >30 ppmv significantly exceed the maximum shifts of 12 ppmv CO_2 found in Antarctic ice. These discrepancies can be explained as an effect of smoothing resulting from diffusion processes in the firn layer at the site of the ice cores. Such processes lead to a reduced signal of the original atmospheric variability and may obscure high-frequency CO_2 variations (31). A modeling exercise, in which raw stomatal frequency data from *Q. robur* leaves were smoothed analogously to natural CO_2 smoothing in the firn, demonstrates that measured CO_2 mixing ratios in the Antarctic D47 core (9) considerably underestimate the actual atmospheric CO_2 variability during the 13th century (32). Apart from smoothing, diffusion is also responsible for a gas–ice age difference in ice cores, resulting in inadequate dating control with age uncertainties of up to 100 years for CO_2 data for the last millennium (11). Unlike ice-based CO_2 records, leaf-based records have the advantage of providing real-time data because the leaf-morphological CO_2 signature becomes permanently fixed at the moment of leaf development and is unaffected by burial processes.

The presence of high-amplitude CO_2 fluctuations as documented by stomatal frequency studies may falsify the IPCC concept that preindustrial temperature variability is constrained by relatively stable atmospheric CO_2 levels (6, 14, 33, 34). A higher degree of CO_2 variability during the last millennium must have resulted in a more prominent role for CO_2 as a forcing factor of air-temperature changes. In this study, the impact of CO_2 changes on preindustrial temperature is reassessed by quantifying the radiative forcing of the alternative CO_2 record

ENVIRONMENTAL SCIENCES

Author contributions: T.B.v.H., F.W.-C., W.M.K., and H.V. designed research; T.B.v.H., F.W.-C., and W.M.K. performed research; T.B.v.H., F.W.-C., W.M.K., and H.V. analyzed data; and T.B.v.H. and H.V. wrote the paper.

The authors declare no conflict of interest.

Freely available online through the PNAS open access option.

‡To whom correspondence should be addressed. E-mail: tom.vanhoof@tno.nl.

This article contains supporting information online at www.pnas.org/cgi/content/full/0807624105/DCSupplemental.

derived from leaves of *Q. robur* and comparing its strength with solar and volcanic forcing components. The analysis focuses on the period between A.D. 1000 and 1500. At least in the Northern Hemisphere, this period includes a prolonged episode of climatic instability marking the transition between relatively warm weather conditions of the Medieval Climatic Optimum to the predominantly cooler conditions of the Little Ice Age (5, 30).

Results and Discussion

We used the rate of CO_2 responsiveness of oak leaves to derive an atmospheric CO_2 record for the first half of the last millennium (Fig. 1). Principal data are listed in supporting information (SI) Table S1. Data from individual sampling points exhibit varied values of standard deviation of stomatal indices (SIs) [0.01–4.04% SI (see *Materials and Methods*) and a mean standard deviation for the whole leaf assemblage of 1.56%]. Uncertainties in predicted CO_2 mixing ratios related to standard deviations of the SI range between 0.03 and 17.94 ppmv, with an average uncertainty for the whole dataset of 6.04 ppmv. However, the magnitude of the standard deviation does not show any unidirectional trends; low and high values are randomly distributed among successive sampling points. Therefore, despite varied uncertainty intervals, mean SI values (Fig. 1*A*) may be confidently applied for reconstructing mean atmospheric CO_2 trends.

Comparable to other stomata-based records (21, 25–28), reconstructed preindustrial CO_2 levels fluctuate between 319.2 and 292.3 ppmv with an average value of 311.4 ppmv. A normalized record is plotted in Fig. 1*C*. Calculated effects of the reconstructed multidecadal CO_2 fluctuations (up to 34 ppmv) on radiative forcing are shown in Fig. 1*E*. A declining trend from A.D. 1000 until A.D. 1200 by 0.5 W/m^2, interrupted by a temporary increase of 0.2 W/m^2 around A.D. 1100, is followed by a prominent increase of 0.7 W/m^2 that occurs between A.D. 1200 and 1300 as a result of a 34 ppmv CO_2 rise. After A.D. 1300 CO_2 forcing declines by 0.4 W/m^2. Calculations derived from the ECBILT-CLIO climate model indicate that the CO_2 changes would result in maximum global temperature anomalies of 0.25°C (Fig. 2).

Although the modeled temperature anomalies remain well within the range of maximum variability recognized by IPCC (6), they are difficult to match with the heterogeneous patterns exhibited by the individual proxy records that have been used to reconstruct time series of surface air-temperature variations on the Northern Hemisphere. Because actual temperature changes are generated by the sum of all forcing components, it is evident from Fig. 1*D* that any direct coupling between trends in atmospheric CO_2 and air temperature between A.D. 1000 and 1500 is likely to be masked by the reconstructed changes in solar forcing as well as by the prominent volcanic event of A.D. 1258 (35).

The supposedly modest atmospheric CO_2 variability during the last millennium recognized in the IPCC *Fourth Assessment Report* is generally related to changes in terrestrial carbon storage and/or variation in CO_2 solubility in the oceans (6, 14, 33, 34). It has been hypothesized that anthropogenic land-cover conversion in particular could have been critical in determining changes in distribution and size of terrestrial carbon sources and sinks (13, 14). Successive pollen assemblages from leaf-bearing sediments have enabled direct temporal correlation of stomata-based proxy CO_2 data and a high-resolution reconstruction of vegetation and medieval land use for the period between A.D. 1000 and 1500 (30). The 13th-century CO_2 increase corresponds to a well known period of massive forest clearing in Europe. In the pollen record, prolonged effects of the mid-14th century plague pandemic, known as the Black Death, are clearly reflected by a period of significant agricultural regression and concomitant reclamation of abandoned farmland by woody vegetation. It is conceivable that the Black Death may have been

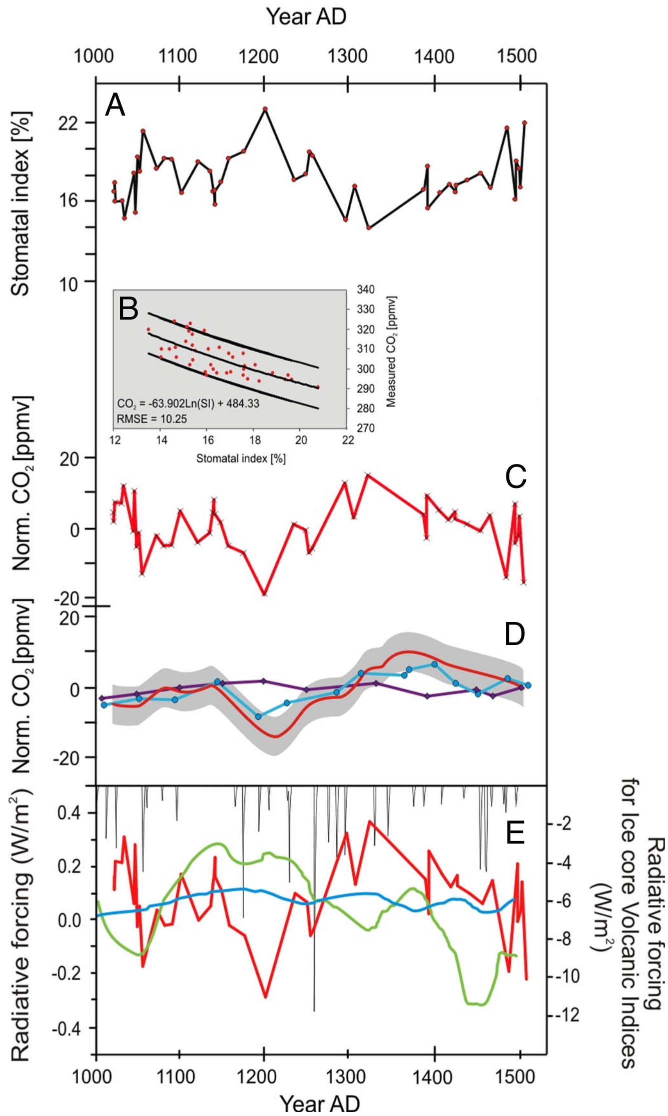

Fig. 1. The CO_2 (SI) record reconstructed for the period A.D. 1000–1500 is compared with Antarctic ice core records and the calculated radiative forcing of this new CO_2 curve is compared with conventional climate forcing factors of the past millennium. (*A*) Stomatal indices of subfossil oak leaves (*Q. robur*) derived from accelerator mass spectrometry ^{14}C wiggle-match dated oxbow-lake deposits from the Netherlands (30). (*B*) SI–CO_2 inference model developed for *Q. robur* based on leaves from herbaria and subrecent peat deposits (22). (*C*) SI-based normalized atmospheric CO_2 fluctuations for the period A.D. 1000–1500. (*D*) Comparison between normalized atmospheric CO_2 reconstructions based on ice core data [light blue line: D47, Antarctica (9); purple line: Law Dome, Antarctica (10)] and the normalized CO_2 (SI) data (*C*) smoothed analogously to the natural CO_2 smoothing in the firn of D47 (red line; gray area represents the methodological error; for details see ref. 32). (*E*) CO_2 (SI) radiative forcing (red line) calculated from the normalized SI-based atmospheric CO_2 curve (*C*) compared with other radiative forcing factors (15–17); CO_2 radiative forcing based on ice core data (blue line), solar forcing (green line), and volcanic forcing (black lines).

a contributing factor to a process of CO_2 decline during the 14th and 15th centuries (30), but modeling exercises suggest that plague-induced carbon storage on land could have accounted for only a CO_2 decrease of not more than $\approx$2 ppmv (14).

Although some of the preindustrial CO_2 changes are at least temporally associated with anthropogenic influences on the environment, the amount of carbon needed to cause a shift of 34 ppmv would far exceed the size of potential carbon sources and

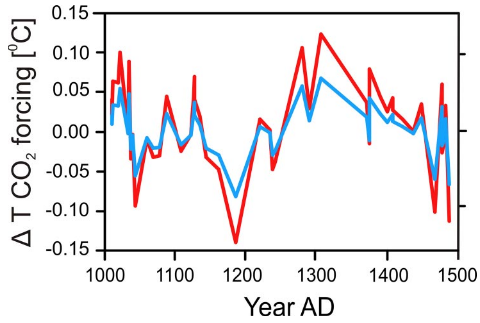

Fig. 2. Estimated global temperature effects on the SI-based CO_2 forcing calculated with a low (blue line) and high (red line) sensitivity mode of the ECBILT-CLIO coupled atmospheric-ocean-sea ice model (43, 45).

sinks in the terrestrial biosphere. It is likely that, analogous to early Holocene CO_2 changes (25–28), depletion and restoration of atmospheric CO_2 between A.D. 1000 and 1500 was driven mainly by short-term perturbations of sea-surface temperature and/or salinity. Similar to the CO_2 trend based on *Tsuga heterophylla* needles (29), within the dating uncertainties, the present stomata-based CO_2 reconstruction correlates to a large extent with proxy sea-surface temperature records from various parts of the North Atlantic Ocean (36–38).

Concluding Remarks

A coherent scenario explaining preindustrial atmospheric CO_2 changes of the last millennium and their possible temporal link with changes in terrestrial and marine carbon uptake or release still needs to be established. Reconstructed multidecadal changes are not as prominent as man-made CO_2 increases since the onset of industrialization. Yet it seems obvious that a dynamic CO_2 regime with fluctuations of up to 34 ppmv implies that CO_2 can no longer be discarded as a forcing factor of preindustrial air-temperature changes. The results of our study therefore underscore the need to understand anthropogenic global warming within the context of rates and amplitudes of natural CO_2 variability of the last millennium. A stomata-based CO_2 record may provide an important observational constraint on the sensitivity of climate models.

Materials and Methods

We based our study on a series of CO_2 estimates derived from well preserved *Q. robur* leaf remains, which occur continually in the organic-rich infill of an oxbow lake of the river Roer near the village of Sint Odiliënberg, Province of Limburg, southeastern part of the Netherlands (51.088 N 6.008 E; for details see ref. 30). The studied leaf record was derived from 60 successive horizons, which were accurately dated by accelerator mass spectrometry ^{14}C wiggle-match dating (for details see ref. 30).

Because of significant differences between the stomatal frequency in sun and shade leaves of *Quercus*, we restricted the analysis to sun morphotypes. Standardized stomatal frequency counts were made by using the image-analysis program analySIS 3.0 (Soft Imaging System) on the digitized images. Parameters measured were (mean) epidermal cell density (ED; number per mm^2) and (mean) stomatal density (SD; number per mm^2). To evade influences of lateral epidermal cell expansion resulting from contrasting light regimes, leaf age, or water availability (39, 40) from SD and ED, the area-independent (mean) SI (41) was calculated as

$$SI[\%] = [SD/(SD + ED)]\cdot 100. \quad [1]$$

Calculated SI values (Fig. 1*A*) are mean values for five leaves per sampling point. Seven images per leaf with a field area of 0.03 mm^2 were analyzed (standard deviations are constant after seven counts). SI values were transferred into CO_2 mixing ratios (Fig. 1*C*) by means of an inference model based on the species-specific stomatal frequency adjustment to the historical atmospheric CO_2 increase of the last ≈150 years. For this model (Fig. 1*B*), SI values of accurately dated *Q. robur* leaves from Dutch herbaria and young peat deposits were compared with the global atmospheric CO_2 trends recognized at Mauna Loa and in shallow Antarctic ice cores (for details see ref. (23), resulting in the following inference model:

$$CO_2[ppmv] = -63.902 \ln(SI) + 484.33. \quad [2]$$

To calculate the strength of radiative forcing induced by the CO_2 changes observed in the Dutch stomatal frequency study, we followed the approach of Myhre *et al.* (42), who expressed the radiative forcing as:

$$dF[W/m^2] = \alpha\cdot\ln(C/CO) + \beta\cdot(\sqrt{C} + \sqrt{CO}), \quad [3]$$

where *dF* represents the radiative forcing, *C* represents the CO_2 mixing ratio, *CO* represents the unperturbed mixing ratio, $\alpha = 5.35$, and $\beta = 0.0906$.

IPCC arbitrarily takes A.D. 1750 as the preindustrial baseline (43). Therefore, to identify changes in radiative forcing induced by the reconstructed CO_2 changes, normalized stomata-derived CO_2 data were superimposed on the corresponding CO_2 reference level of 278 ppmv. It should be noted that, in general, CO_2 data derived from stomatal frequency analysis have higher average values (≈300 ppmv) compared with the IPCC baseline (21, 25–28). Effects of the changes on global air temperatures were estimated with the ECBILT-CLIO coupled atmosphere–ocean–sea ice model (44, 45).

ACKNOWLEDGMENTS. We thank David Dilcher for his continuous and stimulating interest in this work, and Hans Renssen and Hughes Goosse for their invaluable advice with calculating radiative forcing and temperature. We also appreciate the insightful comments of two anonymous reviewers. This study was supported by the Council for Earth and Life Sciences of the Netherlands Organization for Scientific Research. This work is Netherlands Research School of Sedimentary Geology publication no. 2008.09.02.

1. Esper J, Cook ER, Schweingruber FH (2002) Low-frequency signals in long tree-ring chronologies for reconstructing past temperature variability. *Science* 295:2250–2253.
2. Cook ER, Esper J, D'Arrigo RD (2004) Extra-tropical Northern Hemisphere land temperature variability over the past 1000 years. *Quat Sci Rev* 23:2063–2074.
3. Moberg A, Sonechkin DM, Holmgren K, Datsenko NM, Karlén W (2005) Highly variable Northern Hemisphere temperatures reconstructed from low- and high-resolution proxy data. *Nature* 433:613–617.
4. Osborn TJ, Briffa KR (2006) The spatial extent of 20th-century warmth in the context of the past 1200 years. *Science* 311:831–834.
5. Committee on Surface Temperature Reconstructions for the Past 2,000 Years, National Research Council (2006) *Surface Temperature Reconstructions for the Past 2,000 Years* (National Academies Press, Washington, DC).
6. Jansen E, *et al.* (2007) *Climate Change 2007: The Physical Science Basis. Contribution of Working Group I to the Fourth Assessment Report of the Intergovernmental Panel on Climate Change*, eds Solomon S, *et al.* (Cambridge Univ Press, Cambridge, UK), pp 433–497.
7. Intergovernmental Panel on Climate Change (2001) *Climate Change 2001: Synthesis Report. A Contribution of Working Groups I, II, and III to the Third Assessment Report of the Intergovernmental Panel on Climate Change*, eds Watson RT, *et al.* (Cambridge Univ Press, Cambridge, UK).
8. Siegenthaler U, *et al.* (1988) Stable-isotope ratios and concentration of CO_2 in air from polar ice cores. *Ann Glaciol* 10:151–156.
9. Barnola JM, *et al.* (1995) CO_2 evolution during the last millennium as recorded by Antarctic and Greenland ice. *Tellus* 47:264–272.
10. Etheridge DM, *et al.* (1996) Natural and anthropogenic changes in atmospheric CO_2 over the last 1000 years from air in Antarctic ice and firn. *J Geophys Res* 101:4115–4128.
11. Indermühle A, *et al.* (1999) Holocene carbon-cycle dynamics based on CO_2 trapped in ice at Taylor Dome, Antarctica. *Nature* 398:121–126.
12. Siegenthaler U, *et al.* (2005) Supporting evidence from the EPICA Dronning Maud Land ice core for atmospheric CO_2 changes during the past millennium. *Tellus* 57B:51–57.
13. Ruddimann WF (2003) The anthropogenic greenhouse era began thousands of years ago. *Clim Change* 61:261–293.
14. Ruddimann WF (2007) The early anthropogenic hypothesis: Challenges and responses. *Rev Geophys* 45:RG4001.
15. Bard E, Raisbeck G, Yiou F, Jouzel J (2000) Solar irradiance during the last 1200 years based on cosmogenic nuclides. *Tellus* 52B:985–992.
16. Crowley TJ (2000) Causes of climate change over the past 1000 years. *Science* 289:270–277.
17. Bauer E, Claussen M, Brovkin V (2003) Assessing climate forcings of the Earth system for the past millennium. *Geophys Res Lett* 30:1–4.
18. Bradley RS, Briffa KR, Cole JE, Hughes MK, Osborn TJ (2003) *Paleoclimate, Global Change and the Future*, eds Alverson K, Bradley RS, Pedersen TF (Springer, Berlin), pp 105–141.
19. Gray JE, *et al.* (2000) The HIC signalling pathway links CO_2 perception to stomatal development. *Nature* 408:713–715.
20. Wagner F, *et al.* (1996) A natural experiment on plant acclimation: Lifetime stomatal frequency response of an individual tree to annual atmospheric CO_2 increase. *Proc Natl Acad Sci USA* 93:11705–11708.

21. Kouwenberg LLR, *et al.* (2003) Stomatal frequency adjustment of four conifer species to historical changes in atmospheric CO_2. *Am J Bot* 90:610–619.
22. Wagner F, Dilcher DL, Visscher H (2005) Stomatal frequency responses in hardwood-swamp vegetation from Florida during a 60-year continuous CO_2 increase. *Am J Bot* 92:690–695.
23. van Hoof TB, Kürschner WM, Wagner F, Visscher H (2006) Stomatal index response of *Quercus robur* and *Quercus petraea* to the anthropogenic atmospheric CO_2 increase. *Plant Ecol* 183:237–243.
24. Garcia-Amorena I, Wagner F, van Hoof TB, Gomez Manzeneque F (2006) Monitoring the stomatal response to the anthropogenic CO_2 increase in the southern European realm. *Rev Palaeobot Palynol* 141:303–312.
25. Wagner F, *et al.* (1999) Century-scale shifts in Early Holocene CO_2 concentration. *Science* 284:1971–1973.
26. Wagner F, Aaby B, Visscher H (2002) Rapid atmospheric CO_2 changes associated with the 8200-years-B.P. cooling event. *Proc Natl Acad Sci USA* 99:12011–12014.
27. Wagner F, Kouwenberg LLR, van Hoof TB, Visscher H (2004) Reproducibility of Holocene atmospheric CO_2 records based on stomatal frequency. *Quat Sci Rev* 23:1947–1954.
28. Jessen CA, Rundgren M, Björck S, Muscheler R (2007) Climate forced CO_2 variability in the early Holocene: A stomatal frequency reconstruction. *Glob Planet Change* 57:247–260.
29. Kouwenberg LLR, Wagner F, Kürschner WM, Visscher H (2005) Atmospheric CO_2 fluctuations during the last millennium reconstructed by stomatal frequency analysis of *Tsuga heterophylla* needles. *Geology* 33:33–36.
30. van Hoof TB, Bunnik FPM, Waucomont JGM, Kürschner WM, Visscher H (2006) Forest re-growth on medieval farmland after the Black Death pandemic: Implications for atmospheric CO_2 levels. *Palaeogeogr Palaeoclim Palaeoecol* 237:396–411.
31. Trudinger CM, Rayner PJ, Enting IG, Heimann M, Scholze M (2003) Implications of ice core smoothing for inferring CO_2 flux variability. *J Geophys Res Atmos* 108(D16):4492.
32. van Hoof TB, *et al.* (2005) Atmospheric CO_2 during the 13th century AD: Reconciliation of data from ice core measurements and stomatal frequency analysis. *Tellus* 57B:351–355.
33. Gerber S, *et al.* (2003) Constraining temperature variations over the last millennium by comparing simulated and observed atmospheric CO_2. *Clim Dynam* 20:281–299.
34. Joos F, Gerber S, Prentice IC, Otto-Bliesner BL, Valdes PJ (2004) Transient simulations of Holocene atmospheric carbon dioxide and terrestrial carbon since the Last Glacial Maximum. *Glob Biogeochem Cycles* 18:doi:10.1029/2003GB002156.
35. Oppenheimer C (2003) Ice core and palaeoclimatic evidence for the timing and nature of the great mid-13th century volcanic eruption. *Int J Clim* 23:417–426.
36. deMenocal P, Ortiz J, Guilderson T, Sarntheim M (2000) Coherent high- and low-latitude climate variability during the Holocene Warm Period. *Science* 288:2198–2202.
37. Cronin TM, Dwyer GS, Kamiya T, Schwede S, Willard DA (2003) Medieval Warm Period, Little Ice Age and 20th century temperature variability from Chesapeake Bay. *Glob Planet Change* 36:17–29.
38. Eiriksson J, *et al.* (2006) Variability of the North Atlantic Current during the last 2000 years based on shelf bottom water and sea surface temperatures along an open ocean shallow marine transect in western Europe. *Holocene* 16:1017–1029.
39. Poole I, Kürschner WM (1999) *Fossil Plants and Spores: Modern Techniques*, eds Jones TP, Rowe NP (Geol Soc, London), pp 257–260.
40. Royer DL (2001) Stomatal density and stomatal index as indicators of paleoatmospheric CO_2 concentration. *Rev Palaeobot Palynol* 114:1–28.
41. Salisbury EJ (1927) On the causes and ecological significance of stomatal frequency, with special reference to the woodland flora. *Phil Trans R Soc London B* 216:1–65.
42. Myhre G, Highwood EK, Shine KP, Stordal F (1998) New estimates of radiative forcing due to well mixed greenhouse gases. *Geophys Res Lett* 25:2715–2718.
43. Forster P, *et al.* (2007) *Climate Change 2007: The Physical Science Basis. Contribution of Working Group I to the Fourth Assessment Report of the Intergovernmental Panel on Climate Change*, eds Solomon S, *et al.* (Cambridge Univ Press, Cambridge, UK), pp 129–234.
44. Opsteegh JD, Haarsma RJ, Selten FM, Kattenberg A (1998) ECBILT: A dynamic alternative to mixed boundary conditions in ocean models. *Tellus* 50A:348–367.
45. Goosse H, Fichefet T (1999) Importance of ice-ocean interactions for the global ocean circulation: A model study. *J Geophys Res* 104:23337–23355.